Energetics in Plasma Polymerization: Behavior of Various Organic Compounds in Dielectric Barrier Discharges

B. Nisol[1], S. Watson[1], S. Lerouge[2] and M. R. Wertheimer[1]

[1]*Groupe des Couches Minces (GCM) and Department of Engineering Physics, Polytechnique Montréal, Box 6079, Station Centre-Ville, Montreal QC, H3C 3A7, Canada*
[2]*Research Centre, Centre Hospitalier de l'Université de Montréal (CRCHUM), and Department of Mechanical Engineering, École de technologie supérieure (ÉTS), Montréal (Qc), Canada*

Abstract: We report dielectric barrier discharge (DBD)-based atmospheric pressure (AP) plasma polymerization (PP) experiments using argon carrier gas and a wide variety of molecules as the precursors ("monomers"). Electrical measurements yield values of E_m, the energy absorbed from the plasma by each monomer molecule. Systematic differences among families of compounds enable us to draw important conclusions about fragmentation and polymerization in the DBD plasma environment.

Keywords: Atmospheric pressure, dielectric barrier discharge, energetics, polymerization

1. Energy Measurements in AP-PECVD Processes

The plasma-enhanced chemical vapor deposition (PECVD) and -polymerization (PP) literature has long been interested in correlating deposition kinetics, physico-chemical and structural properties of films with the amount of energy absorbed by "monomer" molecules in the plasma, E_m. Before the year 2000, PECVD and PP were mostly carried out under partial vacuum, but atmospheric pressure (AP) plasma processing has since then gained much interest: the absence of costly vacuum installations promises more economical implementation, even though required high carrier gas flows counteract this trend [1-3]. Dielectric barrier discharges (DBD) constitute the main approach for industrial processing [2, 3], such plasmas being obtained in gaps between two electrode surfaces at least one of which is covered by a layer of dielectric. Like LP discharges, they are non-equilibrium (cold) plasmas, and they can be used in various other plasma-chemical applications beside PECVD and PP [4].

Until recently, energy measurements mostly pertained to LP plasmas, where the reagent (monomer) feed is usually undiluted, and where energy absorbed by the discharge can nowadays be evaluated relatively simply and precisely thanks to special dedicated instrumentation. In the case of AP DBD plasmas this is very different, because the discharge must be sustained in a flow of (inert) carrier gas, for example Ar, with typically only parts per thousand (‰) concentrations of monomer. Accurate determination of energy, especially the portion absorbed by the reagent molecules, had not been possible until quite recent work in this laboratory [1, 5-7].

In various articles, these authors have already presented the methodology of energy measurements in DBD plasmas, along with experiments performed on gaseous elements or families of organic compounds. The objective here is to illustrate this research for the case of numerous hydrocarbons, both aliphatic and aromatic, and to generalize the observations in terms of molecular structure.

2. PP of Hydrocarbons: Saturated vs Unsaturated

To avoid repeating information presented earlier [1, 6], we will assume the reader's familiarity with E_m, the energy absorbed from the plasma per monomer molecule, and the method used to measure it. Fig. 1 shows plots of (a) E_m versus F_d, the monomer flow rate (in sccm); and (b) E_m versus $1/F_d$, both for a series of straight-chain alkanes ranging from C1 (methane) to C8 (n-octane). As reported earlier [7, 8], curves in (a) are seen to present the same sets of common features, namely a sharp rise in E_m at small F_d values, followed by a distinct peak [hereafter referred to as $(E_m)_{max}$, the highest value for that particular hydrocarbon, observed at F_d, hereafter designated $(F_d)_{crit}$] and a smooth decrease with rising F_d values. The regions in (a) before and after the peak are respectively referred to as "monomer-lean" and "monomer-rich". In (b) we note a near-linear increase in E_m with rising $1/F_d$; as pointed out earlier [5, 7, 8], this slope in the monomer-rich region is also a characteristic for the particular molecule, and it has units of power (Watts). We note that all slopes appear to be quite similar, values summarized in Table 1, where families of compounds have been listed from top to bottom (alkanes, alkenes, alkynes, aromatics, in that order). Some interesting systematic trends can be observed, for example particularly low $(F_d)_{crit}$ values for most alkanes, and similar slope wattages among members of any given family, in general. Along with what was stated in regard to $(E_m)_{max}$, we believe that these all bear witness to complex plasma-chemical mechanisms that take place within these DBD plasmas.

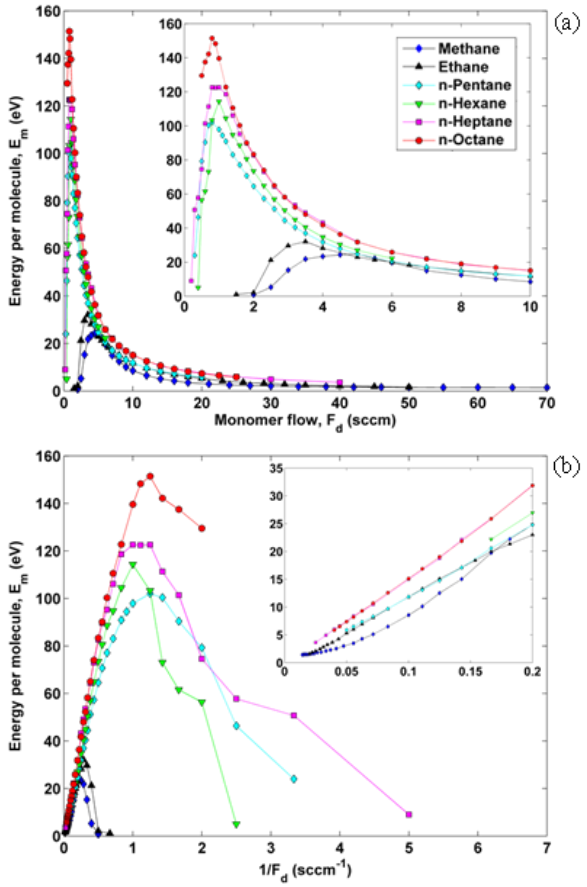

Fig. 1. Plots of (a) E_m (average energy absorbed per molecule in eV, see text) versus F_d; (b) E_m versus $1/F_d$, for seven straight-chain alkane compounds. Adapted from ref. [9].

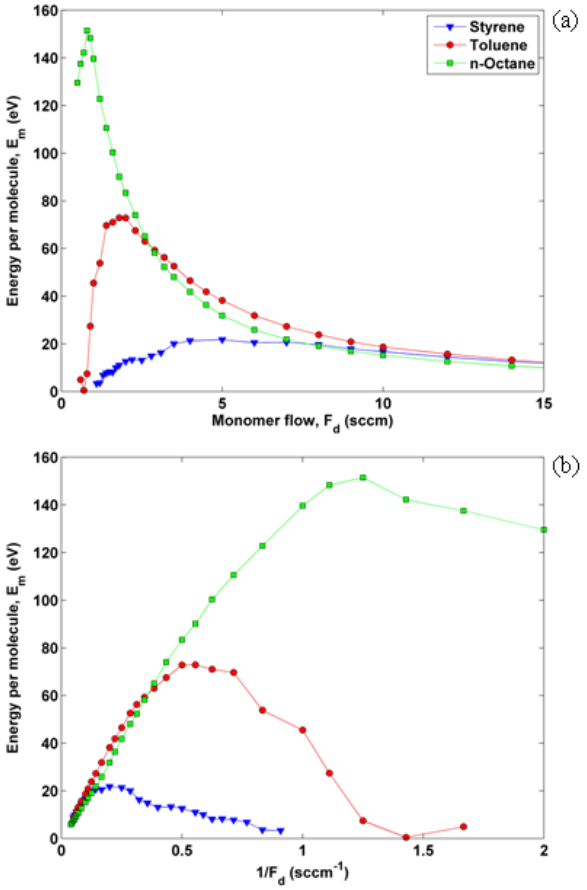

Fig. 2. Plots of (a) E_m versus F_d; (b) E_m versus $1/F_d$, for styrene, toluene and n-octane. Adapted from ref. [9].

Table 1. Numerical values of slopes (in Watts), $(E_m)_{max}$ (in eV), and $(F_d)_{crit}$ (in sccm) for a series of volatile hydrocarbons.

Monomer	Slope [W]	$(E_m)_{max}$ value [eV]	$(F_d)_{crit}$ [sccm]
Methane	2.7	24.8	5
Ethane	8.5	32.1	3.5
n-Pentane	9.4	102.1	0.9
Isopentane	10.4	91.7	1.2
n-Hexane	11.5	114.3	1
Cyclohexane	11.4	104.2	1.2
n-Heptane	11.3	120.6	0.9
n-Octane	14.8	151.4	0.8
Isooctane	10.8	139.3	0.8
Ethylene	12.2	33.9	4
Propylene	12.1	41.7	3.5
1,3-Butadiene	9.3	19.2	4.8
Acetylene	13.0	11.4	14
1-Pentyne	11.1	55.1	1.2
Benzene	13.6	44.6	2.5
Toluene	13.2	72.9	2
o-Xylene	12.9	69.3	1.8
Styrene	9.9	21.7	5

Presuming that more information about plasma-chemical mechanisms can likely be gleaned by examining higher-*M* monomers, Fig. 2 presents three such molecules that have similar high *M* values, namely (1) styrene [104.1 g/mol]; (2) toluene [92.1 g/mol]; and (3) n-octane [114.2 g/mol]. The latter, of course, is a saturated linear hydrocarbon, while (1) and (2) both exhibit aromatic rings. Clearly, the following differences become apparent: $(E_m)_{max}$ values follow the order: n-octane (139.3 eV) ≫ toluene (72.9 eV) ≫ styrene (21.7 eV). In that same order, the transitions between *monomer-rich* and *monomer-lean* regions, i.e. values of $(F_d)_{crit}$, become progressively less well defined: For (1) (styrene), the position of $(E_m)_{max}$ can barely be distinguished, because the peak shape is so extremely broad, but $(F_d)_{crit}$ (see Table 1) rises in the order (3) → (2) → (1).

Finally, Fig. 2(b) and Table 1 reveal quite different slopes for (1), (2) and (3), namely 9.9, 13.2 and 14.8 W, respectively. This systematic increase appears to accompany decreasing unsaturation: comparing styrene (9.9 W) with toluene (13.2 W), despite having similar molecular structures, this appears to underline the role of styrene's vinyl group that raises its plasma reactivity. To further examine these important findings, much smaller $(E_m)_{max}$ and smaller slope values for styrene, we prepared

two series of plasma polymer deposits from the two monomers and conducted a detailed study of their respective FTIR (ATR) spectra (not shown here).

Fig. 3 presents A_{Ar}/A_{Al} as a function of F_d, where A_{Ar} and A_{Al} are the respective areas under the IR absorption bands of the C-H aromatic stretching (3100-3000 cm^{-1}) and of the C-H aliphatic stretching (3000-2800 cm^{-1}) band regions. One immediately notes that A_{Ar}/A_{Al} is significantly higher for PP-styrene than for PP-toluene. Furthermore, the latter ratio drops steadily with diminishing F_d, reaching its lowest value near $(F_d)_{crit}$ [corresponding to $(E_m)_{max}$], while the ratio for PP-styrene appears to remain constant in the *monomer-rich* region, decreasing only when $F_d \leq (F_d)_{crit}$ [$E_m \leq (E_m)_{max}$], that is, within the *monomer-lean* region. This is felt to constitute additional proof that the vinyl group in styrene is the preferred reactive site during plasma polymerization, while for toluene the aromatic ring is disrupted by the plasma under all present experimental conditions. For completeness, we also present on Fig. 3 values of A_{Ar}/A_{Al} for liquid toluene, and from a reference spectrum of atactic polystyrene [10]. These confirm, not surprisingly, that aliphatic features of the corresponding PP come to dominate on account of the well-known cross-linked and/or branched structures of PPs.

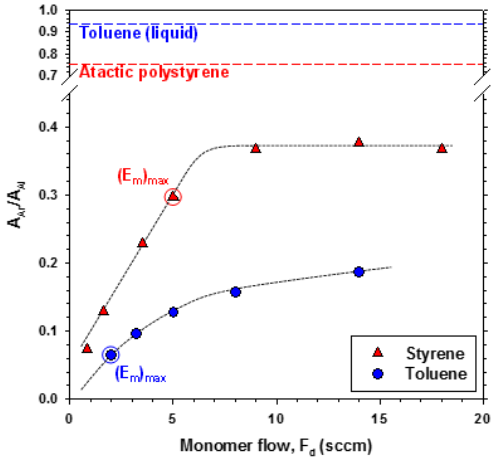

Fig. 3. A_{Ar}/A_{Al} (Area ratio of aromatic over aliphatic C-H stretching) versus F_d for PP-toluene and PP-styrene. The blue and red dotted lines are corresponding pure toluene and atactic polystyrene ratios, respectively. Adapted from ref. [9].

On the basis of ellipsometric measurements, deposition rates, *r*, for (1) styrene, (2) toluene, and (3) n-octane were evaluated and plotted as a function of F_d, as shown in Fig. 4. Over the complete F_d range, *r* values follow similar trends, but with $r_{(1)} \gg r_{(2)} \gg r_{(3)}$. In the plot for octane, *r* is seen to drop gradually with diminishing F_d, but then it drops sharply near $(F_d)_{crit}$ [corresponding to $(E_m)_{max}$] to *r* = 19 nm/min. In contrast, toluene and styrene show local maxima in *r* near their respective $(E_m)_{max}$ values, namely $r_{(2)}$ = 169 nm/min and $r_{(1)}$ = 433 nm/min, respectively. On the basis of ATR FTIR observations, this can be explained by breakage of the aromatic rings that may release up to three highly reactive C=C bonds. When further decreasing F_d, the *monomer-lean* region is reached and *r* suddenly begins to drop, as noted particularly for styrene (blue triangles). Considering a fixed monomer flow rate, say F_d = 0.8 sccm, the *r* value for styrene, *r* = 66 nm/min, is roughly 3 times greater than that for n-octane. The same *r* for n-octane would require F_d = 14 sccm, again illustrating the far greater reactivity of styrene compared with n-octane, the linear saturated hydrocarbon of similar mass, *M*.

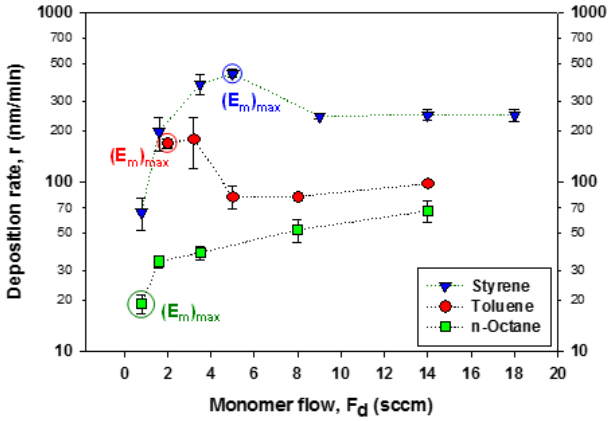

Fig. 4. Deposition rate, *r*, of PP-styrene, PP-toluene and PP-n-octane, plotted versus monomer flow rate, F_d. Note that *r* is plotted on a logarithmic scale. Adapted from ref. [9].

3. Behavior of Various Organic Molecules

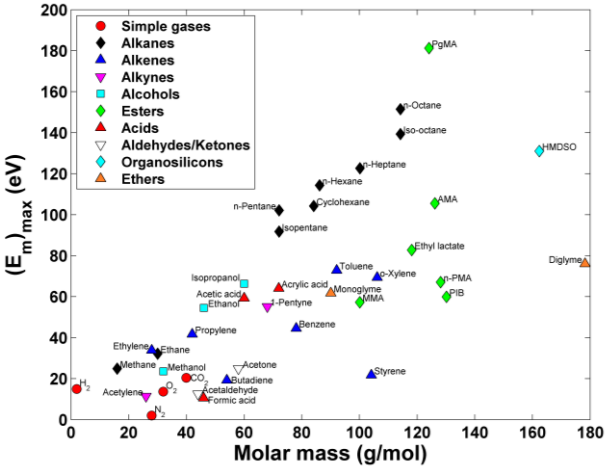

Fig. 5. Plot of $(E_m)_{max}$ (in eV) versus molecular mass, *M*, for a series of simple gases and more complex organic molecules. Explanation of abbreviations: MMA: methyl methacrylate; PIB: propyl isobutyrate; n-PMA: n-propyl methacrylate; AMA: allyl methacrylate; PgMA: propargyl methacrylate; HMDSO: hexamethyldisiloxane (f = 20 kHz, V_a = 2.8 kVrms, F = 10 slm).

The general trend observed indicates that as molar mass increases, so does the corresponding $(E_m)_{max}$. Simple (low-M) gases like H_2, O_2, N_2, CO_2 merely undergo excitation, dissociation or ionization reactions, as reflected by $(E_m)_{max} \leq 20$ eV, while large-M organic compounds display high $(E_m)_{max}$ values.

Now, returning to molecules that incorporate double- or triple bonds, this study has also revealed some exceptions. As noted for the hydrocarbons, where unsaturations yield lower $(E_m)_{max}$, certain other compounds can manifest an opposite trend, one where greater unsaturation results in *higher* $(E_m)_{max}$ values.

This is particularly noteworthy in the family of esters, four of which (all except MMA) possess M values near 130 g/mol. From Fig. 5 one may note similar $(E_m)_{max}$ for MMA, PIB and n-PMA (57.3, 59.9 and 67.1 eV, respectively). For those three compounds, this is believed to correspond to near-total breakage of all constituent covalent bonds [5]. For AMA and PgMA, $(E_m)_{max}$ is particularly high, roughly twice (105.5 eV) or threefold (181.2 eV) greater than the PIB value. The exceptional reactivity of those molecules, attributed to their additional unsaturations, is believed to generate heavier fragments in the discharge, possibly dimers (AMA) and trimers (PgMA) which can also become subject to fragmentation, hence to the possibility of ever-larger measured values of E_m. This, in turn, can be interpreted as a competition between oligomerization and fragmentation, in which case the former mechanism is favored for unsaturated hydrocarbons; yet, the addition of other functional groups, namely esters, can lead to a change in the overall balance.

4. Conclusions

On hand of a variety of hydrocarbon monomers and more complex organic precursors, we have demonstrated the powerful capabilities of accurate energy measurements per molecule, E_m. In principle, knowledge of E_m should enable plasma process design *before* evaluating the ensuing coating properties. This, in turn, can facilitate (i) prediction of outcomes when using new molecular precursors; (ii) reactor scale-up for industrial uses, and (iii) comparison of data from different laboratories. Although the present results have all be obtained with AP DBD plasmas, the latter characteristic, item (iii), has even been shown to apply when comparing AP and low-pressure (LP) processes [11, 12].

Acknowledgments: The authors are grateful for financial support from the Natural Sciences and Engineering Research Council of Canada (NSERC) and from the *Fonds de recherche du Québec – Nature et technologies* (FRQNT) via Plasma Québec. We thank Dr. Hervé Gagnon for valuable technical assistance and Yves Leblanc for skilled technical work.

5. References

[1] B. Nisol, H. Gagnon, S. Lerouge, M. R. Wertheimer, Plasma Processes and Polymers **13,** 366 (2016).
[2] D. Pappas, Journal of Vacuum Science and Technology A **29,** 020801 (17 pp.) (2011).
[3] F. Massines, C. Sarra-Bournet, F. Fanelli, N. Naudé, N. Gherardi, Plasma Processes and Polymers **9,** 1041 (2012).
[4] F. S. Denes, S. Manolache, Progress in Polymer Science **29,** 815 (2004).
[5] S. Watson, B. Nisol, S. Lerouge, M. R. Wertheimer, Langmuir **31,** 10125 (2015).
[6] M. Archambault-Caron, H. Gagnon, B. Nisol, K. Piyakis, M. R. Wertheimer, Plasma Sources Science and Technology **24,** 045004 (16 pp) (2015).
[7] B. Nisol, S. Watson, S. Lerouge, M. R. Wertheimer, Plasma Processes and Polymers **13,** 557 (2016).
[8] B. Nisol, S. Watson, S. Lerouge, M. R. Wertheimer, Plasma Processes and Polymers **13,** 900 (2016).
[9] B. Nisol, S. Watson, S. Lerouge, M. R. Wertheimer, Plasma Processes and Polymers In Press (DOI: 10.1002/ppap.201600191) (2016).
[10] P. Painter, M. Sobkowiak, Y. Park, Macromolecules **40,** 1730 (2007).
[11] D. Hegemann, B. Nisol, S. Watson, M. R. Wertheimer, Plasma Processes and Polymers **13,** 834 (2016).
[12] D. Hegemann, B. Nisol, S. Watson, M. R. Wertheimer, Plasma Chemistry and Plasma Processing In Press (DOI:10.1007/s11090_016_9754_x) (2016).